INVESTIGATION ON THE VACUUM PROPERTIES OF Al-TiZrV Bi-layer FILMS*

X. Y. Jin, T. Guo, X. P. Xu, W. J. Ma, X. S. Zhou, L. Fan, Y. Z. Hong, S. H. Wang†
National Synchrotron Radiation Laboratory, University of Science and Technology of China, Hefei, China

Abstract

Maintaining an ultra-high vacuum (UHV) environment is essential for the Hefei Advanced Light Facility (HALF) to achieve its design performance. Owing to the dimensional limitations imposed by small-aperture vacuum chambers, non-evaporable getter (NEG) films are commonly applied to the inner walls to enhance vacuum performance. However, conventional NEG films increase the resistive-wall impedance of the vacuum pipes, thereby exacerbating the wakefield effects. To address this problem, a novel composite film, Al-TiZrV, has been developed. By covering the TiZrV film surface with a highly conductive film, it can reduce the resistivity of the composite film. The results show that while the addition of the Al layer reduces the resistivity significantly, it increases the secondary electron yield (SEY), exacerbating the electron cloud effect. This study provides insights into the complex properties of similar bilayer films for future research on accelerator-related materials.

INTRODUCTION

In modern particle accelerators, the performance of the vacuum system is critical for maintaining the stability of particle beams. Traditional NEG films, such as TiZrV, are widely used to achieve ultra-high vacuum due to their excellent gas absorption capability [1]. They play a critical role in adsorbing residual gases, and ensuring a stable vacuum environment, all of which are vital for the efficient operation of particle accelerators. However, the TiZrV film has a relatively high resistivity, which may significantly aggravate the resistive-wall impedance of the vacuum chamber. This effect is particularly pronounced in vacuum chambers with small apertures, such as those used in the HALF, where it can lead to beam instabilities. The resistive-wall effects can cause beam emittance growth, energy dispersion, and other undesirable effects, thereby limiting the performance of the accelerator [2].

To address this issue, this research has explored adding an Al layer to the surface of the TiZrV film to suppress the adverse impacts caused by high resistivity [3]. Therefore, a comprehensive investigation of the properties of Al-TiZrV composite films is essential for evaluating their potential in improving the performance of accelerator vacuum systems [4].

* Work supported by the National Natural Science Foundation of China (Grant No. 12175225), the National Key Research and Development Program of China (No. 2023YFA1608602), and the Youth Innovation Promotion Association CAS, China (No. 2023478).

† sihui@ustc.edu.cn

EXPERIMENTAL PROCEDURES

Film Deposition

The Al-TiZrV composite films were deposited via a direct-current magnetron sputtering system. High-purity TiZrV alloy target (99.9% purity, atomic ratio 1:1:1) and Al target (99.9% purity) were utilized. Prior to deposition, oxygen-free copper (OFC) substrates were cleaned using RSB-117 solution, passivated in ammonium citrate solution, and dried with high-purity nitrogen. Silicon wafers were ultrasonically cleaned in acetone solution and dried similarly.

The composite film was commenced with the deposition of the TiZrV film onto the substrates, employing a direct current (DC) magnetron sputtering technique. This initial layer was followed by the sequential deposition of an Al layer. The detailed parameters are shown in Table 1. To systematically vary the thickness of the Al layer, deposition time was precisely controlled at 10, 20, and 30 minutes. To ensure comparability, standalone TiZrV film was also deposited under identical conditions, facilitating a direct assessment of the influence exerted by the Al layer on the characteristics of the composite film.

Table 1: Deposition Parameters

Film	Deposition Time[min]	Current[A]	Working Pressure[Pa]	Gas
TiZrV	180	0.6	1	Ar
Al	10/20/30	0.1	1	Ar

Microstructural Characterization

A scanning electron microscope (SEM) coupled with an energy dispersive X-ray spectrometer (EDS) was utilized to assess the surface morphology and cross-sectional structure of the film. The cross-sections were prepared by cleaving the silicon wafers. The EDS analysis was used to map the elemental distribution within the films, providing insights into the composition and structure of the deposited film.

Secondary Electron Yield Measurement

The secondary electron yield (SEY) measurement setup consists of a sample chamber, an electron gun, a test chamber, and a pumping system, as shown in Fig. 1. The test chamber was pumped to 5×10^{-7} Pa using a 300 L/s turbo-molecular pump and a 200 L/s sputter ion pump. The sample was placed in the sample chamber, pumped to 5×10^{-5} Pa, then transferred to the test chamber by the transfer arm and the pressure of the test chamber should be pumped below 5×10^{-7} Pa for measurement.

An electron beam with energies from 100 eV to 1000 eV and a current of 600 nA was directed at the sample surface. The current was measured by a picoammeter, with initial -40 V bias for secondary electron emission and +70 V for collection. The SEY is the ratio of the number of secondary electrons emitted from a surface, to the number of electrons incident to that surface [5]. Therefore, the SEY (δ) was calculated as Eq. (1).

$$\delta = 1 - \frac{I_t}{I_p}, \tag{1}$$

where I_p is the total primary electron current and I_t is the total current flowing through the sample, measured at +70 V and -40 V.

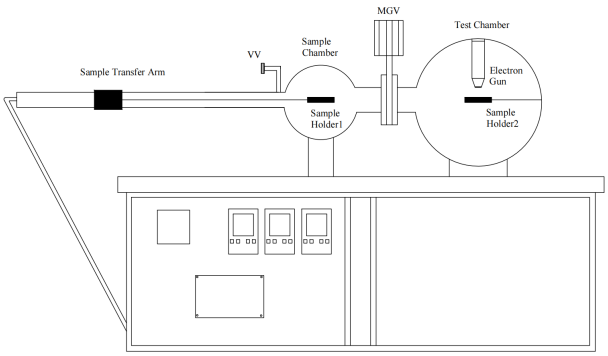

Figure 1: SEY measurement facility.

Resistivity Measurement

The resistivity measurements of the composite films on the copper substrate with different thickness of Al layers, deposited for 10, 20, and 30 minutes, were conducted at room temperature using the four-point probe method with an ST2258C digital four-probe tester. The process involved applying four probes in a linear array to the sample surface, passing a current through two probes, and measuring the voltage across the other two. The resistivity was calculated from the voltage-to-current ratio. This technique was applied to samples with different Al layers to evaluate their resistive characteristics.

RESULTS AND DISCUSSION

Surface Morphologies

The EDS images (Fig. 2) clearly demonstrate that a uniform layer of Al has been successfully deposited onto the surface of the TiZrV film, resulting in a continuous and homogeneous coating. Additionally, other elements are evenly distributed and there is no obvious segregation phenomenon, which is essential to ensure the properties of the composite film.

The SEM images presented in Fig. 3 illustrate the morphological evolution of Al-TiZrV bilayer films at various deposition time, highlighting the surface morphology (a, d, g), TiZrV film thickness (b, e, h), and Al layer thickness (c, f, i). The deposition time significantly impacts both the

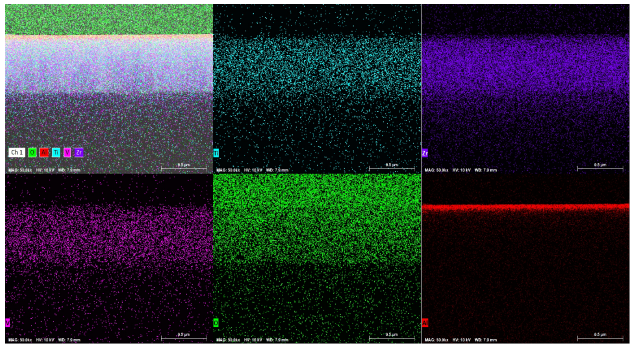

Figure 2: EDS images of Al-TiZrV composite film with Al layer.

surface characteristics and cross-sectional structure of the films. Initially, at a deposition time of 10 minutes, the film surface displays a cauliflower-like texture, likely due to the nucleation of small, irregularly distributed Al particles during the early stages of deposition. As the deposition time extends to 20 minutes, the Al particles begin to gather, filling surface irregularities and leading to a more uniform and smoother surface morphology, indicative of improved Al layer coverage over the TiZrV film. Extending the deposition to 30 minutes results in a higher density of Al particles on the surface, exhibiting a glossy granular structure. Cross-sectional observations reveal that the underlying TiZrV film maintains a columnar structure facilitating the transportation and adsorption of gas molecules, while the overlying Al layer shows a continuous increase in thickness as deposition time extends, potentially altering the physical properties of the composite film.

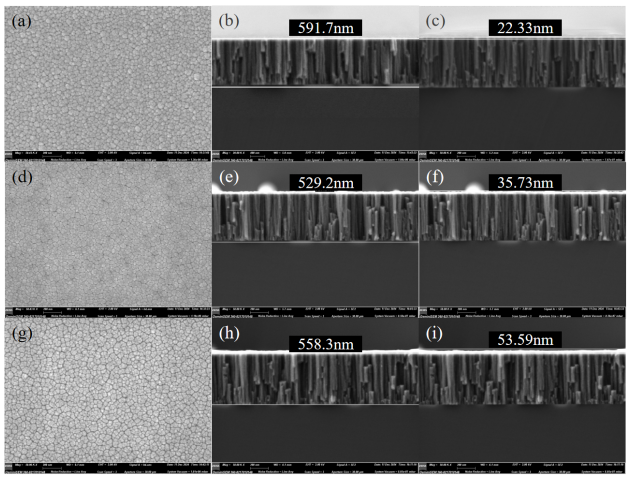

Figure 3: SEM images of Al-TiZrV composite film with Al layer deposition for 10 min (a, b, c), 20 min (d, e, f), and 30 min (g, h, i). (a, d, g) Surface topography; (b, e, h) TiZrV film thickness; (c, f, i) Al layer thickness.

Resistivity of TiZrV film and Al-TiZrV film

The resistivity measurements of the films are shown in Table 2. Upon the deposition of an Al layer, there is a marked reduction in resistivity by approximately two orders of magnitude while the as-deposited TiZrV film exhibits a resistivity

of $4.52 \times 10^{-6}\,\Omega\,\mathrm{m}$. Furthermore, as the thickness of the Al layer increases, the resistivity of the composite film continues to decrease, demonstrating the effectiveness of the Al layer in lowering the electrical resistivity of the composite film. This reduction in resistivity effectively mitigates the resistive-wall effect, a critical factor for optimizing performance in practical applications.

Table 2: Resistivity of Different Al Layers

Film	Al Layer Thickness [nm]	Resistivity [Ω·m]
TiZrV	–	4.52×10^{-6}
Al-TiZrV	22.33	2.64×10^{-8}
Al-TiZrV	35.73	2.57×10^{-8}
Al-TiZrV	53.59	2.45×10^{-8}

SEY of Al-TiZrV films with different Al layers

The SEY of Al-TiZrV composite films was systematically investigated as a function of the Al layer thickness. The results demonstrated a clear correlation between SEY and the thickness of the Al layer. Specifically, the maximum SEY values for films with Al layer deposition time of 10, 20, and 30 minutes were measured to be 2.48, 2.50, and 2.70, respectively, as shown in Fig. 4. This trend indicates that the SEY increases progressively with the thickness of the Al layer, highlighting the influence of Al layer deposition time on the secondary electron emission properties of the composite films.

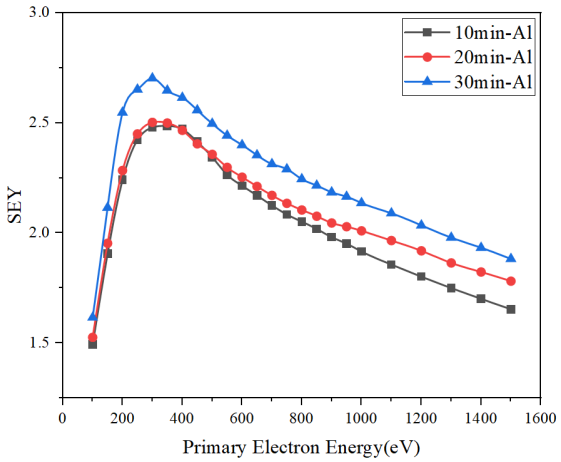

Figure 4: SEY values of Al-TiZrV films with different Al layer thicknesses as a function of electron beam energy.

The increase in SEY with Al layer thickness could be attributed to the intrinsic properties of Al film, which has a relatively high SEY compared to TiZrV film [6]. Additionally, the surface morphology and microstructure of the composite films may also play a role in exacerbating SEY. As the Al layer thickness increases, the surface roughness and the density of nucleation sites may further influence the secondary electron emission [7].

CONCLUSION

In this study, Al-TiZrV composite films were successfully deposited on oxygen-free copper substrates and silicon wafers by magnetron sputtering. Surface characterization confirmed the formation of a well-defined bilayer structure with homogeneous Al coverage, demonstrating the uniform distribution and successful integration of the Al layer.

However, the results of resistivity and SEY measurements indicated a clear trade-off. While the Al layer effectively reduced resistivity by two orders of magnitude, it increased SEY and exacerbated the electron cloud effect in accelerator vacuum systems. Even so, the Al-TiZrV bilayer remains practically useful for accelerator sections where low resistive-wall impedance is prioritized over strict electron-cloud suppression. Future research should focus on mitigating the adverse SEY increase while retaining low resistivity, such as optimizing Al thickness below 20 nm or exploring low-SEY, high-conductivity alternatives (Cu, Ag). This work provides valuable insights for designing low-impedance NEG coatings in accelerator vacuum systems.

REFERENCES

[1] A. M. Al-Khateeb, R. W. Hasse, O. Boine-Frankenheim, W. M. Daqa, and I. Hofmann, "Transverse resistive wall impedances and shielding effectiveness for beam pipes of arbitrary wall thickness", *Phys. Rev. Spec. Top. Accel. Beams*, vol. 10, no. 6, 2007. doi:10.1103/PhysRevSTAB.10.064401

[2] M. Migliorati, E. Belli, and M. Zobov, "Impact of the resistive wall impedance on beam dynamics in the future circular e+e- collider", *Phys. Rev. Accel. Beams*, vol. 21, no. 4, 2018. doi:10.1103/PhysRevAccelBeams.21.041001

[3] K. Yigit *et al.*, "Investigation on activation characterization, secondary electron yield, and surface resistance of novel quinary alloy ti–zr–v–hf–cu non-evaporable getters", *Rev. Sci. Instrum.*, vol. 95, no. 6, 2024. doi:10.1063/5.0198398

[4] X. Jin *et al.*, "Innovative fabrication and comparative analysis of tizrv single and cu–tizrv bilayer films", *Nuclear Instruments and Methods in Physics Research Section A: Accelerators, Spectrometers, Detectors and Associated Equipment*, vol. 1072, p. 170242, 2025. doi:10.1016/j.nima.2025.170242

[5] J. Wang, Y. Wang, Y. Xu, B. Zhang, and W. Wei, "Research on the secondary electron yield of tizrv-pd thin film coatings", *Vacuum*, vol. 131, pp. 81–88, 2016. doi:10.1016/j.vacuum.2016.05.001

[6] W. Cao *et al.*, "Secondary electron emission characteristics of the al2o3/mgo double-layer structure prepared by atomic layer deposition", *Ceram. Int.*, vol. 47, no. 7, pp. 9866–9872, 2021. doi:10.1016/j.ceramint.2020.12.128

[7] Y. Wu *et al.*, "Secondary electron yield (sey) evolution of laser processed oxygen-free high conductivity copper induced by different ultrasonic cleaning durations", *Vacuum*, vol. 221, p. 112891, 2024. doi:10.1016/j.vacuum.2023.112891